The Starburst-Interstellar Medium Interaction in NGC 1569
I. Location and Nature of He II Sources Using *Hubble Space Telescope WFPC2* Imagery[1]

Brent A. Buckalew and Reginald J. Dufour

Rice University, Department of Space Physics & Astronomy,
Houston, TX 77025, USA
Email: `brent@regultra.rice.edu`, `rjd@rice.edu`

and

Patrick L. Shopbell

California Institute of Technology, Department of Astronomy, MC 105-24
Pasadena, CA 91125, USA
Email: `pls@astro.caltech.edu`

and

Donald K. Walter

South Carolina State University, Department of Physical Sciences,
Orangeburg, SC 29117, USA
Email: `dkw@physics.scsu.edu`

ABSTRACT

We present the detection of He II sources in the Im galaxy NGC 1569 from *HST WFPC2* imagery. Out of the fifteen detections, seven were Wolf-Rayet stars, five were stellar clusters with associated He II emission, and three were sources of unknown origin. The detected Wolf-Rayet stars' colors and magnitudes are similar to Large Magellanic Cloud late-type WN stars. The physical origin of the other He II sources are discussed. We conclude that the equivalent of 51$\pm$19 WNL stars have been detected in NGC 1569, and we have estimated the total Wolf-Rayet population in NGC 1569 as 78$\pm$51. These numbers are compared with the Wolf-Rayet stellar populations in the SMC, LMC, Milky Way, and other starburst galaxies relative to their luminosities, dynamical masses, and ionized gas masses.

Previous to this study, Wolf-Rayet stars in NGC 1569 were not detected using ground-based imagery, but were only indicated through longslit spectroscopy. This

[1]Based on observations with the NASA/ESA *Hubble Space Telescope*, obtained at the Space Telescope Science Institute, which is operated by AURA, Inc., under NASA contract NAS5-26555.

is the first time the exact locations of the Wolf-Rayet stars in this nearby, well-studied, "post-starburst" galaxy have been determined.

Subject headings: galaxies: individual (NGC 1569) — galaxies: stellar content — stars: Wolf-Rayet

1. Introduction

Evidence of large numbers of Wolf-Rayet (WR) stars in galaxies serves as a tracer of recent starbursts. The locations of WR stars indicate where star formation occurred $\lesssim$ 10 Myr ago and where OB stars of mass $\gtrsim$ 20 $M_\odot$ evolved to this state (e.g., Schaerer et al. 1999 and references therein). From the numbers and locations of such stars, one can determine the starburst properties and can study the kinematical and morphological impact the starburst has on the interstellar medium (ISM). Such studies are particularly important in dwarf irregular galaxies because of their low escape velocity ($\sim$ 100 km s^{-1}; Drissen, Roy, & Moffat 1993). Because starburst galaxies have large star formation rates (e.g., log $\Sigma_{\rm SFR} \approx -0.8$ $M_\odot$ yr^{-1} kpc^{-2}; Kennicutt 1998), the number of massive stars is enhanced. With the detection of massive WR stars in these disturbed systems, it is possible to correlate the morphology of the gas (both H I and H II) and the recent star formation history.

NGC 1569 is a nearby (D = 2.2$\pm$0.6 Mpc; Israel 1988) Im galaxy that has been well-studied over the last 20 years. Two prominent, stellar-like features are located at the center of this galaxy, which are thought to be super-star clusters (SSCs; cf. Prada, Greve, & McKeith 1994) formed in a starburst 2-10 Myr ago (González-Delgado et al. 1997). It is speculated that they will evolve into globular clusters. Recent results suggest that SSC A is two stellar clusters superimposed on one another (De Marchi et al. 1997). Identifying 45 clusters within NGC 1569, Hunter et al. (2000) determined their ages which range from 2 Myr to 1 Gyr, and they found a subconcentration of clusters, including SSC A, had an age of 4-5 Myr old.

From multiwavelength studies the gaseous morphology of NGC 1569 shows evidence of high supernovae activity. Several studies using optical interference-filter imagery of the ionized gas show evidence of an eruptive event which occurred in the galaxy's past (Hodge 1974; de Vaucouleurs, de Vaucouleurs, & Pence 1974; Waller 1991; Hunter, Hawley, & Gallagher 1993; Devost, Roy, & Drissen 1997). Kinematics of the ionized gas that were studied by Tomita, Outa, & Saitou (1994) showed the expanding gas moves at speeds from 10 to 100 km s^{-1}. Heckman et al. (1995) found that the optical filaments at distances of 2 kpc from the center of the galaxy are traveling over 200 km s^{-1}. In the infrared, Hunter et al. (1989) observed the dust radiating warmer at 60-155 μm, which is explained by the starburst's strong radiation field, than dust in similar, irregular galaxies. Radio observations also show relics of the eruptive starburst. Israel & de Bruyn (1988) deduced a high frequency cutoff at 8$\pm$1 GHz, which they attributed to a decrease in relativistic electron injection about 5 Myr ago. Observations of H I (Reakes 1980; Israel & van Driel 1990; Stil & Israel

1998) revealed that the distribution of neutral hydrogen is a clumpy ridge or disk surrounded by arms which mimic the Hα arms seen in the optical. An H I hole was detected surrounding the SSCs and was formed after the starburst (Israel & van Driel 1990). The distribution of the global CO emission is similar to the H I distribution (Young, Gallagher, & Hunter 1984). High resolution CO maps show large (compared to ones in the Galaxy) giant molecular clouds surrounding the SSC A H I hole (Taylor et al. 1999). Finally, ROSAT PSPC and HRI images show an extended soft X-ray component perpendicular to the major axis of the galaxy (Heckman et al. 1995; Stevens & Strickland 1998). ASCA images of a hard X-ray source inside NGC 1569 were interpreted as either low-mass X-ray binaries or young supernova remnants (Della Ceca et al. 1996).

The consensus of these studies is that a starburst occurred approximately 10 Myr ago. This event (of unknown origin) produced SSC A and B. However, companions found around dwarf irregular systems are common (e.g., Taylor et al. 1995). Stil & Israel (1998) have found a 7×10^6 $M_\odot$ companion 5 kpc from NGC 1569, which makes it a possible explanation for what triggered the starburst. There are large numbers of OB and/or WR stars in the two clusters and the surrounding field. Because of the numbers of massive stars and their rapid evolution (first giving rise to stellar winds and then supernovae), the galaxy underwent a pronounced kinematical and morphological change, even disruption, during the past several Myr. Evidence suggests that the supernova ejected material will escape the galaxy and will enrich the intergalactic medium.

Previously, evidence of WR stars in NGC 1569 came primarily from spectroscopic studies. Using this method, WR stars were located in the ring nebula to the far East in the galaxy (Drissen, Roy, & Moffat 1993), in SSC A (González-Delgado et al. 1997), and elsewhere within NGC 1569 (Ho, Filippenko, & Sargent 1995; Martin & Kennicutt 1997). However, Kobulnicky & Skillman (1997; hereafter KS97) found that most of the galaxy's He II λ4686 emission was nebular and their slit locations covered some of the regions where WR stars were previously detected. Ground-based narrow-band λ4686 filter imagery of NGC 1569 was attempted with little success in finding WR stars (e.g., one stellar knot with a light He II λ4686 excess; Drissen, Roy, & Moffat 1993).

With the improvement of spatial resolution of the Hubble Space Telescope over ground-based instruments, it is possible to study the morphology of the ionized gas with higher detail and locate weak stellar He II emission-line sources. In this paper, new HST *WFPC2* F469N filter images are presented in an attempt to locate WR stellar activity and to confirm the previous WR detections. The observations and data reduction are presented in §2 with the basic results of that analysis given in §3. Discussion of the implications of our findings is given in §4. In §5 a summary of our findings and concluding remarks are made.

2. Observations and Reduction

WFPC2 images of NGC 1569 were taken 23 September 1999 for the Cycle 8 program, GO-8133. NGC 1569 was oriented in two of the wide-field chips (WF2 & WF3) of the camera with a nearby 10^{th} magnitude star placed out of the field of view (see Figure 1). The effective plate scale is $0\overset{''}{.}0996$ pixel^{-1} (1.07 pc pixel^{-1} at the adopted distance of 2.2 Mpc). The GO-8133 images used here were F469N (He II), F502N ([O III]), and F547M ($\sim$ Strömgren y). NGC 1569's radial velocity is -104 km s^{-1}. The shift of each emission line is $\sim$ 2 Å, and therefore, all emission lines were observed very near the center of the filter transmission curve. Observational parameters for these data are found in Table 1.

These data were recalibrated using the best reference files and the new STScI "on-the-fly" calibration (OTFC) system. OTFC images gave the same image statistics over the wide-field chips compared to the manually calibrated ones. Additionally, we used OTFC processed archival *WFPC2* imagery of NGC 1569 from the Cycle 6 programs GO-6111 and GO-6423, which were primarily broadband images in *UBVR*. Please refer to Greggio et al. (1998) for more details on the GO-6111 imagery and to Hunter et al. (2000) for discussion of the GO-6423 imagery. Table 1 has observational parameters for these data as well.

The GO-6111 data were dithered by a few pixels for a subset of four exposures. These images needed to be aligned with respect to one another, which was done using standard IRAF[2] applications. For all images, cosmic rays were best removed by using the STSDAS package *crrej*. The cosmic ray removed images were then rotated (in the case of the Cycle 6 data) and aligned with respect to the Cycle 8 F547M image. The F502N and F469N images were continuum subtracted. The total counts of several bright field stars were determined in the F547M, F502N, and F469N images. Average ratios of the emission line to continuum total counts for these stars were found, scaled to the F547M image, and the new F547M image was subtracted from each interference-filter image. This process was iterated until the field stars were subtracted out, and the residuals were at average levels of the background noise.

Drissen et al. (1999) used a weighted average between F547M and F439W images for continuum subtraction of their F469N image of NGC 2403. They indicated that this would properly subtract red stars and not leave them as "holes" if only the F547M were employed. We attempted this method and found that the weighting heavily favored F547M ($\sim$99%), and thus, only F547M was used. Furthermore, the only F439W (GO-6111) image covers one-half of the galaxy on our field.

Flux calibration of our continuum-subtracted, interference-filter images was done using the *WFPC2* exposure time calculator found at STScI's home page. A generic flux of 1.0×10^{-16} ergs cm^{-2} s^{-1}, an exposure time of 1000 seconds, and the redshift velocity of NGC 1569 (-104 km s^{-1}) were inputted to determine the number of object electrons for the F469N and F502N filters. The number of electrons sec^{-1} was converted to DN sec^{-1}, and setting the DN sec^{-1} value equal to the generic flux of 1.0×10^{-16} ergs cm^{-2} s^{-1}, we solved for the flux in one DN sec^{-1}. These conversion numbers are in units of ergs cm^{-2} s^{-1} DN^{-1} and are 1.084×10^{-14} for F502N and 1.847×10^{-14}

[2]IRAF is distributed by the National Optical Astronomy Observatories, which are operated by the Association of Universities for Research in Astronomy, Inc., under cooperative agreement with the National Science Foundation.

for F469N.

With the calibrated He II image, we determined whether the He II emission was due to a WR star, nebular source, or associated with a stellar cluster. All pixels with counts over 3 times the deviation in the background (3σ) in the F469N image were noted as possible detections. Each pixel with apparent emission was carefully checked in the individual F469N exposures to see whether the location had been struck by a cosmic ray, warm pixel or defect which might account for it being high. There was also the possibility that the pixel had a blemish in the continuum image which also might account for it being high. If a pixel location was in any of these categories, it was thrown out. What remained after this rejection process was considered a "good" detection.

Each pixel that met the above criteria was superimposed on the F502N and F555W images. We determined from the superposition whether a good detection's location corresponded to a bright, point-like source in one or both of the images. The detections meeting the requirement of being a point source in F502N but no corresponding point-source in F555W were not found in our search. If the good detection had a corresponding point source in F555W but not in F502N, it was labeled S (for stellar sources) or C (for cluster sources). If the good detection was not associated with any point source in either of the images, it was labeled U in the figures and tables below.

For the S and C sources, the He II flux and *WFPC2* B and V magnitudes were calculated. *WFPC2* B magnitudes were not measured for some sources because the GO-6111 images did not cover some He II locations, or the corresponding point in the F439W image had low signal-to-noise. Our magnitude and search criteria were based on the IRAF procedure *apphot*. The He II pixel location of each S source was chosen as the starting position for the brightest pixel search in the B and V images. The search radius was restricted to within 2 pixels of the He II location. The apertures for the stellar sources were 2 pixels because most of the He II pixels were concentrated in the crowded stellar region of the galaxy. Background counts were taken from an annulus that was one pixel outside the aperture. The number of pixel centers found within the 2 pixel aperture were counted and the total number of counts was computed. The He II flux was found by using the same IRAF program and parameters, and the total counts were converted to an absolute flux. The same procedure was used in the case of the C sources, except the aperture was set to a larger value. Looking at the F555W images, one visually inspected the maximum radius of each cluster, and the average radius was 5 pixels. SSC A was set at 10 pixels, and the background annulus was appropriately expanded. Only the He II flux was found for the U sources, although the procedures were the same as for the S sources.

The absolute emission line fluxes and BV magnitudes presented in Tables 2 through 4 have not been corrected for reddening. Devost, Roy, & Drissen (1997) infer line-of-sight extinction due to the Galaxy in the direction of NGC 1569 is E(B-V) = 0.50 (A_V = 1.6 mag), and the mean intrinsic extinction of NGC 1569 is E(B-V) = 0.20 (A_V = 0.6 mag). We will adopt these values for this study. Using these numbers along with the extinction curve from Seaton (1979), we found the $f(\lambda)$ value of 0.042 for He II and the reddening correction of 11.8. To correct the V and B magnitudes, a value of 28.9 mag must be subtracted to produce an absolute magnitude. This number was computed using the equation

$$(V - M_V)_{\mathrm{NGC1569}} = 5\log(\mathrm{D}) - 5 + \mathrm{A}_V \quad (1)$$

where D is the adopted distance to NGC 1569, A_V is the visual extinction and V is the *WFPC2* F555W magnitude measured. Please note that the magnitudes are F555W and F439W magnitudes based on the STScI "Vega" system and are not true Johnson B and V magnitudes.

3. Imagery Results

Several candidates were found, which can be characterized into three categories. There are seven He II sources which are associated with a stellar source (hereafter, labeled S), five with a cluster (labeled C), and three which are found to have none of the above but are real He II sources (labeled U). Figure 2 shows the locations of the S, C, and U sources (circles) with respect to the rest of the galaxy. The underlying gray-scaled image is F555W (net exposure time = 930 s) from GO-6423.

Figures 3 and 4 show "postage stamp" enlargements of each individual S source, Figure 5 shows each C source, and the U sources are found in Figure 6. The gray-scaled image is the F555W image and the contours are He II for that particular source. Each F555W image has been smoothed using the IRAF command *magnify.* This has made the images more presentable. However, the small continuum sources are too blurred in some cases to see. The contours are set at 60%, 40%, 20%, and 10% of the peak He II flux in all C sources excluding C3 and are set at 100%, 80%, 60%, and 40% in C3 and all S and U sources. All figures are $3''\!.1$ by $3''\!.1$, and the orientation of each image is the same as Figure 1.

4. Discussion

4.1. Global Properties of Sources

We now compare our absolute magnitudes and colors of the NGC 1569 WR stars (S sources; Table 2) to averaged Large Magellanic Cloud (LMC) WR stellar magnitudes and colors taken from Feitzinger & Isserstedt (1983). The comparison with LMC stars is a logical assumption since NGC 1569 is classified as Im and their metallicities are similar. Average S absolute visual magnitudes (M_V = -7.43) best agree with average late-type WN magnitudes (M_V = -6.26 & $(\mathrm{B-V})_o$ = -0.07; Feitzinger & Isserstedt 1983). The colors of the S sources ($(\mathrm{B-V})_o$ = -0.2) are comparable with early-type WN stars (M_V = -4.39 & $(\mathrm{B-V})_o$ = -0.22; Feitzinger & Isserstedt 1983). However, the uncertainties due to high reddening and to measured magnitudes allow for the agreement of colors of the LMC WNL WR stars and S sources. Therefore, we hypothesize that these S sources are similar to LMC WNL stars. Spectroscopy of the individual sources would need to be performed in order to classify each WR star.

The He II luminosity of each S source was checked to Galactic and LMC WR stellar luminosities (2.6×10^{35} – 2.9×10^{36} ergs s^{-1}; Drissen et al. 1999 and references therein). For reference, the average He II luminosity for an early-type WN (WNE) WR star is $5.2\pm2.7\times10^{35}$ ergs s^{-1} and $1.6\pm1.5\times10^{36}$for a late-type WN WR star (Schaerer & Vacca 1998 and references therein). We find all S sources to have similar luminosities to the Galactic and LMC WR stars with S3 (L(He II) $= 4.76\times10^{35}$ ergs s^{-1}) at the lower end of the luminosities and S2 (L(He II) $= 2.04\times10^{36}$ ergs s^{-1}) at the top. S3 and S4 have He II luminosities similar to the average WNE He II luminosity reported by Schaerer & Vacca (1998), and all other S sources are 1σ outside of this value. Massey & Hunter (1998a) find that 30 Doradus has several O3If* stars which were thought to be WN stars in previous surveys. These stars also emit He II and have absolute visual magnitudes similar to our S sources. However, the He II equivalent width of Of stars is typically around 5-10 Å (Nota et al. 1996), and Crowther & Dessart (1998) state a He II luminosity of 1.7×10^{35} ergs s^{-1} for one O3If*/WN star. Schaerer & Vacca (1998 and references therein) also report a He II luminosity for Of stars of 2.5×10^{35} ergs s^{-1}. This amount is a factor of 2 smaller than the faintest S source in He II. Furthermore, the detection of O3 stars would suggest an age $\sim$ 1 Myr (Massey & Hunter 1998a), which contradicts the most recent ages calculated for the clusters in NGC 1569 (4-6 Myr; Hunter et al. 2000). Also, our sensitivity limit of three times the standard deviation of the mean background gives a minimum He II luminosity of 2.4×10^{35} ergs s^{-1} which places the weakest WR stars and Of stars at our detection threshold. We must conclude that the S sources are Wolf-Rayet stars (most likely WN stars), but spectroscopy will have to be performed to determine their spectral type.

From Figure 2 we see that the stellar sources are concentrated close to SSC A. This supports the idea that the most recent starbursting region is primarily concentrated around the super-star clusters A & B. The number of WR stars surrounding SSC A is greater compared to SSC B (5 versus 1). González-Delgado et al. (1997) did not find WR signatures in the spectra around SSC B and Kobulnicky and Skillman (1997; cf. their Figure 1) have spectra over these locations and over most of the stellar sources listed here. They find nebular He II in those spectra only. This leads us to suspect that some of the point sources and He II emission are coincidental, or that the star is photoionizing the interstellar medium to produce He II. However, Conti (1999) brings up a valid point in that some starburst galaxies with the same age do not show WR stars and this could be explained by the fact that continuum dilution of the background starlight could mask over the broad, faint WR emission lines. Since these spectra came from ground-based observatories and the slit used in both papers was wide ($\geq 1\farcs5$), it is possible that continuum dilution overwhelmed the He II emission from these WR stars in one or both cases. Finally, the Wolf-Rayet star spectroscopically discovered by Drissen & Roy (1994) is our S7.

Four of the clusters are also found (see Figure 2) in the largest region of star formation. One cluster is on the Eastern outskirts of the large star formation region. The four clusters within the starburst show both red stars and WR stars (see Figure 5). The reason we know that there are red stars comes from Drissen et al. (1999). They reported that F469N - F555W would produce "holes" where red stars were, and typically there are "holes" at the center of each cluster. Thus, the red stars are separated from the He II emission. This was first reported in De Marchi et al. (1997) as a superposition of two clusters which make up SSC A. In Figure 1 of their paper, they label the West cluster SSC A1 and the East SSC A2 (the orientation of their figure and ours is roughly the same; see our C4 in Figure 5d). SSC A1 is slightly redder than SSC A2. In our He II contours, this splitting is also seen. We find that SSC A2 is where the strongest He II emission is while SSC A1 is centered around the "hole" in the He II contours. This detection of red supergiants along with Wolf-Rayet stars has been well reported in the past and is consistent with the evolution of massive stars (e.g., Massey 1999).

The locations of the "unknown sources" are plotted in Figure 2. The three U sources surround SSC A. This region is filled with He II emission which is similar in surface brightness and may be related to stellar wind-shocks, or even supernova(e). Therefore, it is likely that these He II emissions are nebular in origin. Using the Galactic and LMC He II luminosities above, we see that the He II emission of the unknown sources is comparable (see our Table 4).

4.2. Notes on Individual Sources

Below, comments are given on each of the detections that were reported in Tables 2 through 4 and shown in Figures 3 through 6.

S1 – Figure 3a – One of the more easily discernible stars detected. It is easy to see that the He II emission is coincident with a bright continuum point source.

S2 – Figure 3b – This star is to the West of SSC A. The star is blended with SSC A due to the use of the IRAF *magnify* command. However, it is the brightest of the WR stellar candidates.

S3 – Figure 3c – A star due North of SSC A whose He II emission is the lowest of the WR candidates. The reason for this low amount of emission might be because the internal reddening around this star is larger than the average intrinsic reddening in NGC 1569.

S4 – Figure 3d – Again, another WR star that is close to SSC A and has a low He II emission compared to the other candidates. The arguments for S3 can be applied here.

S5 – Figure 4a – A WR star that is Northeast of SSC A. The He II emission is coincident with the bright point source underneath.

S6 – Figure 4b – This He II source is close to the star and is probably associated with it given the errors in image shifting and rotating. It is the only WR star close to SSC B. The He II emission is comparable to Galactic and LMC WR stars.

S7 – Figure 4c – The WR star found spectroscopically by Drissen & Roy (1994). It is at the larger, brighter source of continuum light in the F555W image. As was stated in their article, the ring nebula was probably the result of the stellar wind from the WR star and its progenitor. There are other point sources inside the bubble which could be associated with the nebula as well and therefore, helped to contribute to the shell's expansion.

C1 – Figure 5a – A cluster within the large H II region West of SSC A. The cluster has two distinct portions. The Southern part has the associated He II emission, and the Northern portion contains several red stars. It is impossible to know whether they are associated or coincident. Recall that KS97 have spectra showing nebular He II over this region. Therefore, we conclude that C1's He II emission is primarily nebular in origin covering an area of 0.0794 arcsec^2, but there could be WR stars lost in KS97's spectra due to continuum dilution. However, if we assume that all the emission is due to WR stars, the number of WNL equivalent stars (using 1.7×10^{36} ergs s^{-1} for the He II flux of an average WNL star from Vacca & Conti 1992) is three. This is cluster 10 in Hunter et al. (2000) and our M_{F555W} magnitude agrees with theirs given the uncertainties in both measurements.

C2 – Figure 5b – A cluster lying Southwest of SSC A. This also has the separation between red stars and He II emission. The red stars are found at the center of the cluster while the brightest He II is at its Eastern edge. The He II emission is equivalent to four WNLs and has an area of 0.0893 arcsec^2. Also, the colors of the system (and C1) are predominantly influenced by red stars. This is cluster 13 in Hunter et al. (2000) and our M_{F555W} magnitude agrees with theirs given the uncertainties in both measurements.

C3 – Figure 5c – Another cluster where the strongest continuum source is a "hole" in the He II image signifying red stars. The peak of He II emission is found to the Northeast of the brightest continuum pixel and has an area of 0.0496 arcsec^2. Also, there is a slight rise in the [O III] flux near the peak He II and gives strong evidence for a nebular origin. KS97's spectra also cover this region which they find only nebular emission. However, if one assumes that all the emission is from WR stars and using the same average emission of a WNL star, the number of WNL equivalents is two. This is not classified as a detected cluster in Hunter et al. (2000).

C4 – Figure 5d – SSC A. González-Delgado et al. (1997) report the finding of 25-40 WNL equivalent stars in SSC A. However, if one uses our numbers and assumes that all the emission is from WR stars, the number of WNL equivalents is $\sim$50. This number is larger than their estimate and suggests that there is some nebular component (with a maximum area of 0.823 arcsec^2) that we cannot separate in this study. However, continuum dilution of the broad λ4686 emission line might be a problem in the González-Delgado et al. (1997) spectra. Thus, the number must be somewhere between the two numbers, probably nearer their estimate. This is cluster A in Hunter et al. (2000) and our M_{F555W} magnitude agrees with theirs given the uncertainties in both measurements.

C5 – Figure 5e – A cluster on the very edge of the starburst and may not be a part of the starburst which created SSC A and its surroundings. Interestingly, this cluster has no red stellar population within or near it. It is the only cluster like this and is far removed from the other four clusters. If one assumes that all the He II emission is from WR stars, the number of WNL equivalent stars is three, similar in number to C1–C3. However, the area of emission is much smaller at 0.0298 arcsec^2. This is cluster 39 in Hunter et al. (2000) and our M_{F555W} magnitude agrees with theirs given the uncertainties in both measurements.

U1 – Figure 6a – The banana-shaped contour is where the maximum level of emission is. It is on the Southern edge of SSC A and is South of S2. The emission is probably nebular in origin with an area of 0.00992 arcsec^2, but the He II emission is similar to the average He II emission of Galactic or LMC WR stars.

U2 – Figure 6b – The cluster to the North (V = 18.1; B-V = 0.63) of U2 has a large population of red stars. Thus, this He II emission might be related to the group of stars just like the situation in the clusters. Therefore, it is possible that one WR star is adjacent to the cluster. However, since no star is seen its nebular origin is more realistic (with an area of 0.0198 arcsec^2).

U3 – Figure 6c – The circular point source is surrounded by three bright clusters. No stellar point sources are found between the three. The emission is most probably nebular in origin, but could be a WR star since the He II emission is comparable to the average He II emission of Galactic or LMC WR stars.

4.3. On the Origin of Nebular He II in NGC 1569

The presence of nebular He II outside of planetary nebulae is rare because few thermal sources produce enough photons with energies > 54 eV. Garnett et al. (1991) stated three alternative ionizing mechanisms which could account for this nebular He II. Hot stellar ionizing continua is a definite possibility for this galaxy. The starburst which produced the WR stars in SSC A occurred only 2-3 Myr ago (González-Delgado et al. 1997) or 4-5 Myr ago (Hunter et al. 2000). Schaerer & Vacca (1998) modeled strong nebular He II due to massive stars in the early starburst phases. These models have been subsequently updated (Schaerer 2000). Using the I(He II 4686)/I(Hβ) ratios from KS97 (their Table 2; values of 8×10^{-3} and 1.2×10^{-2}) and Figure 8 from Schaerer (2000), we conclude that the burst age must be 3-4 Myr old. This is in fair agreement with the younger age of the two-stage burst proposed by González-Delgado et al. (1997) and the recently calculated ages of SSC A and surrounding clusters (Hunter et al. 2000).

The second mechanism for the formation of He II is shock excitation such that the strength of the nebular He II depends on the velocity of the shock: ($V_{\rm shock} \approx 120$ km s^{-1}; Garnett et al. 1991). If shocks were present, bright [O III] emission would be at the same location which may have been seen for C3. At this time, based on our limited imagery, shocks cannot be considered a viable source. Photoionization by X-rays is the final, alternative explanation for nebular He II. Pakull & Angebault (1986) found that nebular He II was produced around the black hole candidate binary LMC X-1. Della Ceca et al. (1996) state that NGC 1569's hard X-ray spectra is due to the two bright X-ray point sources located in the ROSAT high resolution imager data. These sources could be interpreted as low-mass X-ray binaries or young supernova remnants. Future X-ray images would resolve whether these point sources are X-ray binaries and coincident with some of the He II sources stated here. Chandra observations of this object were taken May 2000, and we will have to wait and see whether this hypothesis is valid. Preliminary findings of the Chandra data do not show X-ray binaries coincident with any of our He II sources (Kobulnicky 2000).

4.4. Estimate of the Total Number of Wolf-Rayet Stars in NGC 1569

It was unlikely that we detected all WR stars within NGC 1569, since many are "blurred" into SSC A, and this method principally detects WN stars. We derived a total number of detected Wolf-Rayet stars from our data to be 51±19. This was primarily based on the equivalent number of WNL stars in the C sources. For deriving the minimum number of WR stars in NGC 1569, we assumed that all He II emission in the C sources was nebular unless previously identified as due to WR stars. Then, we took the minimum number of equivalent WNL stars of SSC A (25; González-Delgado et al. 1997) and the individual WR stars found in this paper (7). For the maximum number of WR stars in NGC 1569, we assumed that all He II emission in the C sources was due to WR stars. Because we did not know exactly what type of WR stars produce the He II emission, we determined the equivalent number of WNL stars within each cluster. The total flux of a C source was converted to a luminosity, divided by the average He II luminosity of a WNL star (using 1.7×10^{36} ergs s^{-1} from Vacca & Conti 1992), and the number (truncated to an integer) gave the equivalent number of WNL stars for that C source. This was discussed in Section 4.2, which gave the equivalent number of WNL stars for each C source. Thus, we took the maximum number of equivalent WNL stars of SSC A (50; this paper), the equivalent number of WNL stars in the other C sources (12) and the individual WR stars (7) to arrive at our detected number and range.

If we assume that all the nebular He II is produced from the ionizing continua of massive stars, then we can estimate the total number of WR stars in NGC 1569. Using the values of I(He II 4686)/I(Hβ) from KS97 along with the updated Figure 9 from Schaerer (2000), we can determine the total number of stars. In the last section, we discussed a probable age of the clusters as 3-4 Myr. Over this age range, the ratio of WNL/Total WR stars is 0.65±0.35. Dividing the number of detected WR stars by this percentage gives us an indication of the total number of WR stars within NGC 1569. Within roughly a factor of two, the total number of WR stars in NGC 1569 comes out to be 78±51. The updated figures of Schaerer & Vacca (1998) were corrected for an error in the normalization of the fluxes from WR atmosphere models. Using the old Figure 9 of Schaerer & Vacca (1998), the ratio of WNL/Total WR stars was 0.3±0.3 which gave an estimated total WR number of 160±60. This amount of WR stars is similar to the number of observed WR stars in the LMC. Whereas, the updated model gives a total number closer to the detected amount.

4.5. Comparisons with Other Galaxies

It is useful to compare the estimated numbers of WR stars in NGC 1569 with those for similar galaxies as a function of galaxy properties such as luminosity, total mass (dynamical), and ionized gas mass. This we do in Figures 7-9. The data used in the production of these figures came from several sources. References where we obtained the number of WR stars in the various galaxies were the following: Massey et al. (1992); Vacca & Conti (1992); van der Hucht (1996); Izotov et al. (1997); Massey & Johnson (1998b); Bransford et al. (1999); Breysacher, Azzopardi, & Testor (1999); Drissen et al. (1999); van der Hucht (1999); Guseva et al. (2000). Absolute magnitudes were readily available in several papers (de Vaucouleurs & Pence 1978; Thuan & Martin 1981; Bergvall & Olofsson 1986; Thronson et al. 1990; Kobulnicky et al. 1995; Guseva et al. 2000) and the NASA/IPAC Extragalactic Database. However, limited data could only be found on the total (dynamical) masses (de Vaucouleurs 1960; Burns & Roberts 1971; Cottrell 1976; Loiseau & Bajaja 1981; Thuan & Martin 1981; Jackson et al. 1987; Dufour & Hester 1990; Taylor et al. 1993; Kobulnicky et al. 1995; Stil & Israel 1998; Wilkinson & Evans 1999) and ionized hydrogen masses (Viallefond & Goss 1986; Dufour & Hester 1990; Sivan et al. 1990; Thronson et al. 1990; van den Broek et al. 1991; Waller 1991; Vacca & Conti 1992; Walterbros & Braun 1994; Kennicutt et al. 1995; Mendez et al. 1999; Guseva et al. 2000). Since there are so many sources and different combinations of data for the ordinate and abscissa values, we have not labeled the various data points with different symbols. Because we have two values (detected and estimated total) of the number of WR stars in NGC 1569, we have plotted both in Figures 7-9. The enlarged, solid NGC 1569 datum point is the detected number of WR stars, and the enlarged, hollow NGC 1569 datum point is the estimated total number of WR stars.

Figure 7 plots the number of WR stars detected versus the absolute blue (or photographic) magnitudes of Wolf-Rayet, starburst, and spiral galaxies. The ordinate error bars on the NGC 1569 data points indicate our estimate of the uncertainty due to complications of the nebular He II detected in the galaxy and the estimation procedure for the total number of WR stars as explained in the previous section. The ordinate error bars for a majority of the points comes from using the Guseva et al. (2000) data because they find the number of WNL stars with various emission lines. NGC 2403's ordinate error bars are because Drissen et al. (1999) report 25-40 individual WR stars. The abscissa error bars of a majority of the points come from using the absolute photographic magnitude (M_{pg}) from Guseva et al. (2000). We are assuming that their M_{pg} is ± 1 of M_B. From the figure, one finds a well defined linear correlation between the logarithm of the WR stellar count and absolute blue magnitude for a majority of the Wolf-Rayet galaxies. This is not surprising, for one would expect a correlation between the blue luminosity and the number of WR stars, since WR stars and their O progenitors dominate the blue luminosity of star-forming galaxies. However, both NGC 1569 points are found below the general trend, which could be due to either *(a)* NGC 1569 is a post-starburst galaxy for which most of the recently formed massive stars have already evolved through the WR phase, or *(b)* our estimated number of WR stars in NGC 1569 is too low (i.e., no one has detected WC stars in NGC 1569). We suspect that *(a)* is the more likely reason, and that the SMC might be a similar post-starburst system since the numbers of WR stars in it are rather accurately known. Such might not be the case for estimates of WR stars in the Milky Way and NGC 2403 spirals, which are galaxies likely to have a more uniform recent star formation rate than starbursting irregulars.

Figure 8 is a plot of the number of WR stars versus total mass of galaxies, using a more limited number of good data available in the literature, and Figure 7 ordinate error bars are used here for the correlated data. This graph, albeit quite sparse on good data for the galaxy masses, suggests that total galaxy mass is not a good tracer of the observable number of WR stars in galaxies. This is not surprising since the total galaxy mass includes dark matter, which does not relate directly to recent star formation, and the number of WR stars seen in a galaxy depends critically on the recent star formation efficiency. Star formation efficiency would possibly make a better correlator because several of the small galaxies plotted here are producing similar numbers of WR stars compared to NGC 1569 and the LMC. Five galaxies (SMC, IC 10, NGC 2403, Mrk 178, and Mrk 209) all seem to have a relatively low level of recent star formation efficiency.

Finally, Figure 9 is a plot of the number of WR stars versus the ionized hydrogen (H II) mass, and the Figure 7 ordinate error bars are again used here for the correlated data. This graph, though again sparse on good data for other WR galaxies, shows a positive relation between the number of Wolf-Rayet stars and the mass of H II (given such a conclusion is strongly weighted on the SMC and IC 10). Such is not surprising, given that the young clusters containing WR stars also contain prodigious numbers of O-stars which ionize the surrounding gas. The abscissa lower limits derived from spectral properties in (Guseva et al. 2000) also follow this trend. Several of the lower limits fall within the good data and could signify that the majority of the ionized hydrogen mass fell within the slit. The two lower limits at the right were probably slit locations over larger Markarian galaxies.

The comparisons between NGC 1569 and other WR and nearby galaxies shown in Figures 7-9 further support the idea that NGC 1569 is seen to be in a "post-starburst" phase, but has had a major, even eruptive, *very recent* starburst. While the mass of NGC 1569 is $\sim$30 times less than the LMC, it has approximately similar numbers of WR stars, similar blue luminosity, and a larger H II mass. By comparison with the SMC and IC 10, which have similar to slightly higher dynamical masses, they have fewer WR stars compared to NGC 1569. This, coupled with the extensive system of ionized filaments seen in NGC 1569 (Heckman et al. 1995), suggests that the magnitude of the very recent ($\sim$10 Myr) starburst in NGC 1569 was exceptional. Today, the numbers of WR stars and H II mass found for NGC 1569 reflect the relatively recent end of this starburst, compared to other nearby, star-forming Im galaxies of comparable mass like the SMC and IC 10. In this respect, NGC 1569 still retains the properties of starbursting blue-compact dwarf galaxies compared to typical irregular (Im) systems. Possibly in another 50 Myr or so, NGC 1569 will have properties more similar to the SMC, IC 10, and other irregular systems of similar mass.

5. Summary

Using *HST WFPC2* imagery, we find the following on the morphology and location of He II sources in the post-starburst galaxy NGC 1569.

1. Seven He II sources are associated with a star, indicating that they are WR stars. The four WR stars with both magnitudes and colors are consistent with LMC WN stars. Spectroscopy of the individual WR stars will be performed to confirm their spectral class.

2. Five clusters have associated He II. All clusters (excluding SSC A) have emission which would be due to 2-4 WNL equivalent WR stars. SSC A, which was discovered by González-Delgado et al. (1997) to have 25-40 WNL equivalent WR stars, has about 50 WNL equivalents according to our study.

3. De Marchi et al. (1997) showed that SSC A was a superposition of two separate clusters. We have shown the redder of their two clusters (SSC A1) is the location of a higher concentration of red supergiants, and the WR stars are more concentrated in SSC A2. The coexistence of these two populations is consistent with massive stellar evolution.

4. Three sources close to SSC A were unidentified. The interpretation for these sources is that the emission is nebular in origin and possibly related to SSC A. However, all three have He II emission comparable to the WR stars detected in this survey.

5. The total detected number of WR stars in NGC 1569 is 51±19.The estimated total number of WR stars in NGC 1569 is 78±51.

If some of these sources are nebular in origin, they could be attributed to either hot stellar ionizing continua (which requires the presence of WR stars in most models) or photoionization due to X-rays. Presently, preliminary analysis of the Chandra observations of this object do not show any of our sources near X-ray sources. However, the model of Schaerer & Vacca (1998) and data from KS97 derive similar starburst ages to those from previous and recent stellar models. Therefore, a majority of the nebular He II is associated with the ionizing continua of the massive stars.

This paper is the first in a series of papers on the morphological interaction between the starburst and interstellar medium of NGC 1569. Using other *WFPC2* interference-filter images, we will examine next the detailed morphology of the ionized gas components. The excitation mechanisms of the ionized gas will be modeled both empirically and theoretically, and compared with the neutral and molecular gas distribution.

We would like to thank the referee for his/her insightful comments and suggestions. We would also like to thank Henry Kobulnicky for allowing us to look at his thesis spectra of NGC 1569. B.B.'s research is supported by a NASA-GSRP fellowship (NGT 2-52252). Obtaining the HST observations and funding for R.J.D., P.L.S., and D.K.W. via grants related to the Cycle 8 General

Observer Program GO-8133 were supported by AURA/STScI.

REFERENCES

Bergvall, N. & Oloffson, K. 1986, A&AS, 64, 469

Breysacher, J., Azzopardi, M., & Testor, G. 1999, A&AS, 137, 117

Bransford, M., Thiker, D., Walterbros, R., & King, N. 1999, AJ, 118, 1635

van den Broek, A., van Driel, W., de Jong, T., Lub, J., de Grijp, M., & Goudfrouij, P. 1991, A&AS, 91, 61

Burns, W. & Roberts, M. 1971, ApJ, 166, 265

Conti, P. 1999, IAU Symposium No. 193, *Wolf-Rayet Phenomena in Massive Stars and Starburst Galaxies*, van der Hucht, K., Koenigsberger, G., & Eenens, P., eds. pp. 507-516

Cottrell, G. 1976, MNRAS, 177, 463

Crowther, P. & Dessart, L. 1998, MNRAS, 296, 622

Della Ceca, R., Griffiths, R., Heckman, T., &MacKenty, J. 1996, ApJ, 469, 662

De Marchi, G., Clampin, M., Greggio, L., Leitherer, C., Nota, A., & Tosi, M. 1997, ApJ, 479, 27

Devost, D., Roy, J., & Drissen, L. 1997, ApJ, 482, 765

Drissen, L., Roy, J., & Moffat, A.1993, AJ, 106, 1460

Drissen, L. & Roy, J. 1994, PASP, 106, 974

Drissen, L., Roy, J., Moffat, A., & Shara, M. 1999, AJ, 117, 1249

Dufour, R. & Hester, J. 1990, ApJ, 350, 149

Feitzinger, J. & Isserstedt, J. 1983, A&AS, 51, 505

Garnett, D., Kennicutt, Jr., R., Chu, Y., & Skillman, E. 1991, ApJ, 373, 458

González-Delgado, R., Leitherer, C., Heckman, T., & Cerviño, M. 1997, ApJ, 483, 705

Greggio, L., Tosi, M., Clampin, M.,De Marchi, G., Leitherer, C., Nota, A., & Sirianni, M. 1998, ApJ, 504, 725

Guseva, N., Izotov, Y., & Thuan, T. 2000, ApJ, 531, 776

Heckman, T., Dahlem, M., Lehnert, M., Fabbiano, G., Gilmore, D., & Waller, W. 1995, ApJ, 448, 98

Ho, L., Filippenko, A., & Sargent, W. 1995,ApJS, 98, 477

Hodge, P. 1974, ApJ, 191, 21

van der Hucht, K. 1996, Ap&SS, 238, 1

van der Hucht, K. 1999, IAU Symposium No. 193, *Wolf-Rayet Phenomena in Massive Stars and Starburst Galaxies*, van der Hucht, K., Koenigsberger, G., & Eenens, P., eds. pp. 13-20

Hunter, D., Thronson, Jr., H., Casey, S., & Harper, D. 1989, ApJ, 341, 697

Hunter, D., Hawley, W., & Gallagher III, J. 1993, AJ, 106, 179

Hunter, D., O'Connell, R., Gallagher, J., & Smecker-Hane, T. 2000, AJ, in press

Israel, F. 1988, A&A, 194, 24

Israel, F. & de Bruyn, A. 1988, A&A, 198, 109

Israel, F., & van Driel, W. 1990, A&A, 236, 323

Izotov, Y., Foltz, C., Green, R., Guseva, N., & Thuan, T. 1997, ApJ, 487, 371

Jackson, J., Barrett, A., Armstrong, J., & Ho, P. 1987, AJ, 93, 531

Kennicutt, Jr., R. 1988, ApJ, 334, 144

Kennicutt, Jr., R., Bresolin, F., Bomans, D., Bothun, G., & Thompson, I. 1995, AJ, 109, 594

Kennicutt, Jr., R. 1998, ApJ, 498, 541

Kobulnicky, H., Dickey, J., Sargent, A., Hogg, D., & Conti, P. 1995, AJ, 110, 116

Kobulnicky, H., & Skillman, E. 1997, ApJ, 489, 636

Kobulnicky, H. 2000, private communication

Loiseau, N. & Bajaja, E. 1981, RMxAA, 6, 55L

Martin, C., & Kennicutt, R., Jr. 1997, ApJ, 483, 698

Massey, P., Armandroff, T., & Conti, P. 1992, AJ, 103, 1159

Massey, P. & Hunter, D. 1998a, ApJ, 493, 180

Massey, P. & Johnson, O. 1998b, ApJ, 505, 793

Massey, P. 1999, IAU Symposium No. 193, *Wolf-Rayet Phenomena in Massive Stars and Starburst Galaxies*, van der Hucht, K., Koenigsberger, G., & Eenens, P., eds. pp. 429-438

Mendez, D., Cairos, L., Esteban, C., & Vilchey, J. 1999, AJ, 117, 1688

Nota, A., Pasquali, A., Drissen, L., Leitherer, C., Robert, C., Moffat, A. & Schmutz, W. 1996, ApJS, 102, 383

Pakull, M. & Angebault, L. 1986, Nature, 322, 511

Prada, F., Greve, A., &McKeith, C. 1994, A&A, 288, 396

Reakes, M. 1980, MNRAS, 192, 297

Schaerer, D. & Vacca, W. 1998, ApJ, 497, 618

Schaerer, D., Contini, T., & Pindao, M. 1999, A&AS, 136, 35

Schaerer, D. 2000, private communication

Seaton, M. 1979, MNRAS, 187, 73P

Sivan, J., Petit, H., Comte, G., & Maucherat, A. 1990, A&A, 237, 23

Stevens, I. & Strickland, D. 1998, MNRAS, 301, 215

Stil, J., & Israel, F. 1998, A&A, 337, 64

Taylor, C., Brinks, E., & Skillman, E. 1993, AJ, 105, 128

Taylor, C., Brinks, E., Grashuis, R., & Skillman, E. 1995, ApJ, 99, 427

Taylor, C., Hüttemeister, S., Klein, U., & Greve, A. 1999, A&A, 349, 424

Thuan, T. & Martin, G. 1981, ApJ, 247, 823

Thronson, H., Hunter, D., Casey, S., & Harper, D. 1990, ApJ, 355, 94

Tomita, A., Outa, K., & Saitou, M.1994, PASJ, 46, 335

Vacca, W. & Conti, P. 1992, ApJ, 401, 543

de Vaucouleurs, G. 1960, ApJ, 137, 265

de Vaucouleurs, G.,de Vaucouleurs, A., & Pence, W. 1974, ApJ, 194, 119

de Vaucouleurs, G. & Pence, W. 1978, AJ, 83, 1163

Viallefond, F. & Goss, W. 1986, A&A, 154, 357

Waller, W. 1991, ApJ, 370, 144

Walterbros, R. & Braun, R. 1994, ApJ, 431, 156

Wilkinson, M. & Evans, N. 1999, MNRAS, 310, 645

Young, J., Gallagher, J., & Hunter, D.1984, ApJ, 276, 476

This preprint was prepared with the AAS $\LaTeX$ macros v5.0.

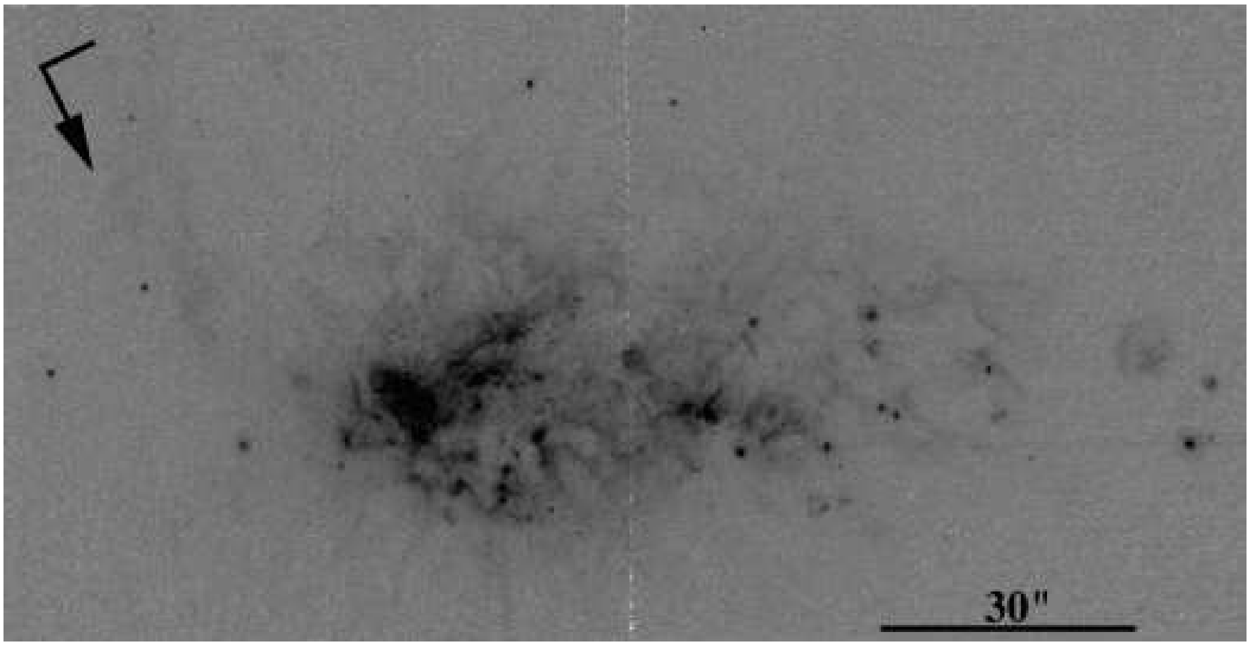

Fig. 1.— [O III] image of NGC 1569 taken 23 September 1999 for GO-8133. HST was oriented so that NGC 1569 fell onto the WF2 and WF3 wide-field chips which left a 10^{th} magnitude star outside the field of view. The orientation of all figures throughout this paper will be the same as this Figure. The field of view is $148'' \times 76''$ (1.579×0.811 kpc).

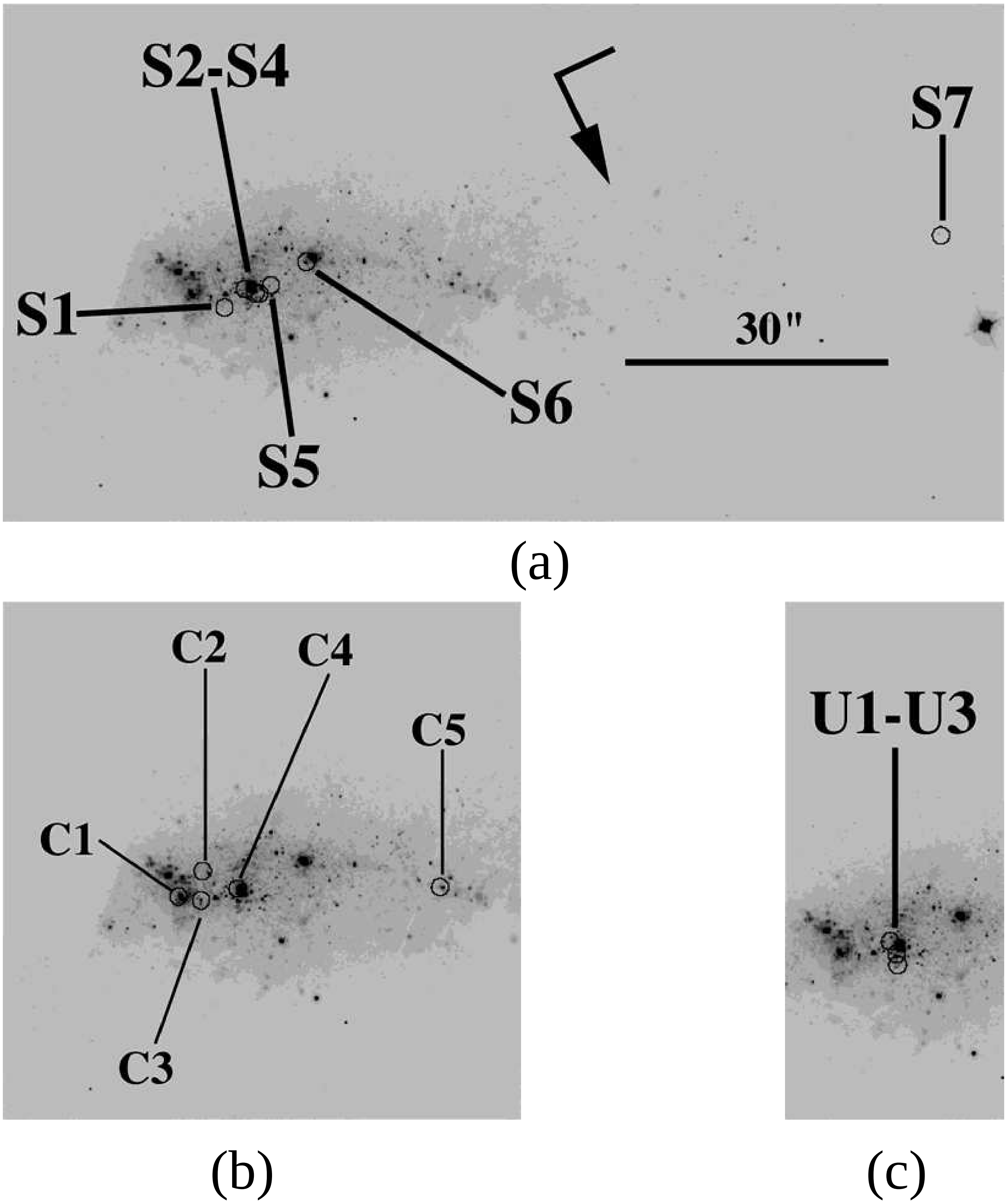

Fig. 2.— Visual continuum images of NGC 1569 taken for GO-6423 with the locations of our He II sources encircled. (a) The Wolf-Rayet candidates (S sources) are identified and labeled as they appear in Table 2. (b) The clusters with associated He II emission (C sources) are identified and labeled as they appear in Table 3. (c) The He II with neither associated [O III] nor visual continuum (U sources) are identified and labeled as they appear in Table 4. All images in this Figure are oriented and scaled as indicated in part (a).

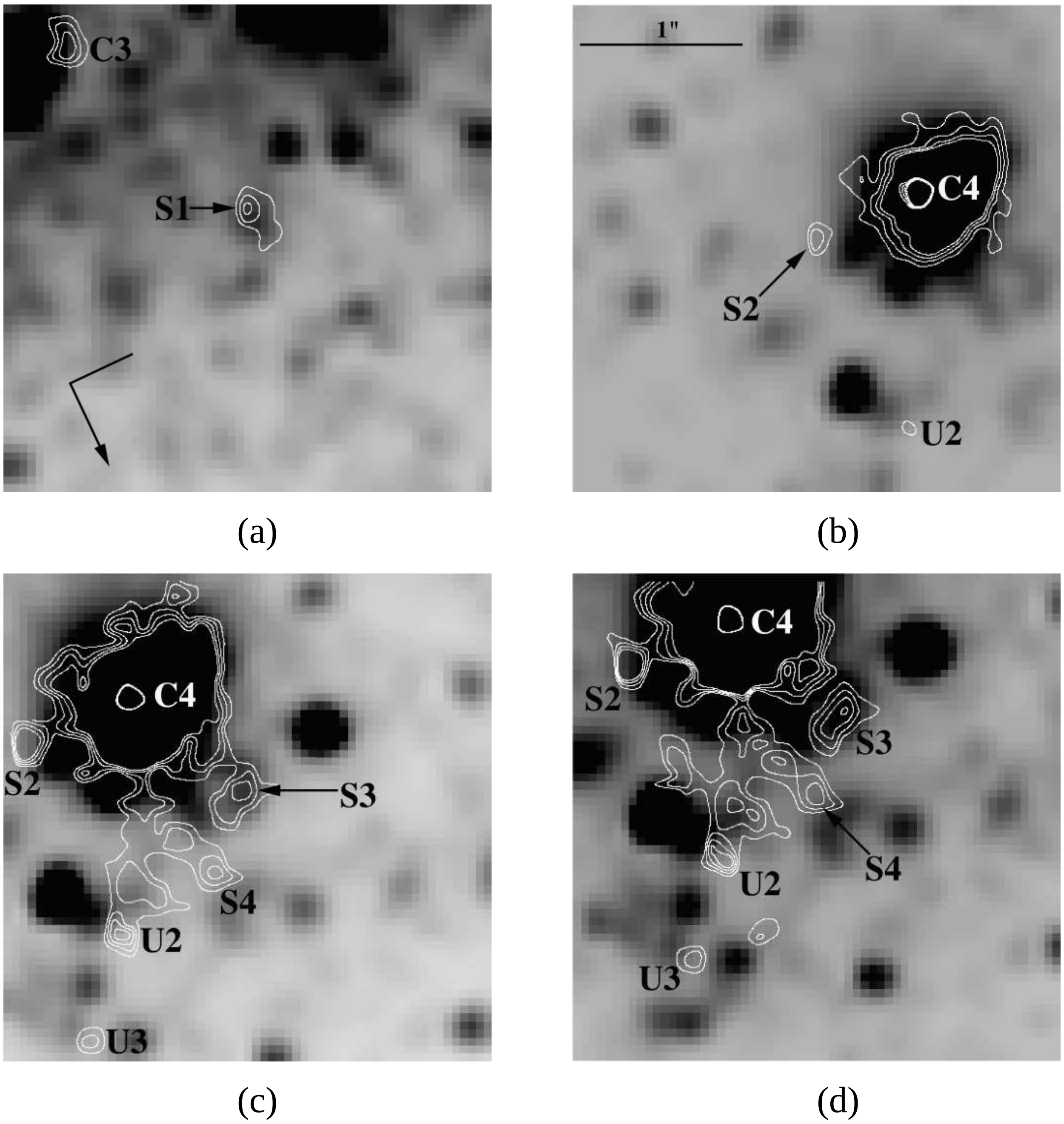

Fig. 3.— "Postage stamp" enlargements of the fields of S objects 1 through 4. The size of each image is $3''.1 \times 3''.1$. The gray-scaled image is F555W and the contours are of the F469N image of the same area. The contours are plotted as the 100%, 80%, 60%, and 40% level of the peak He II emission for that object.

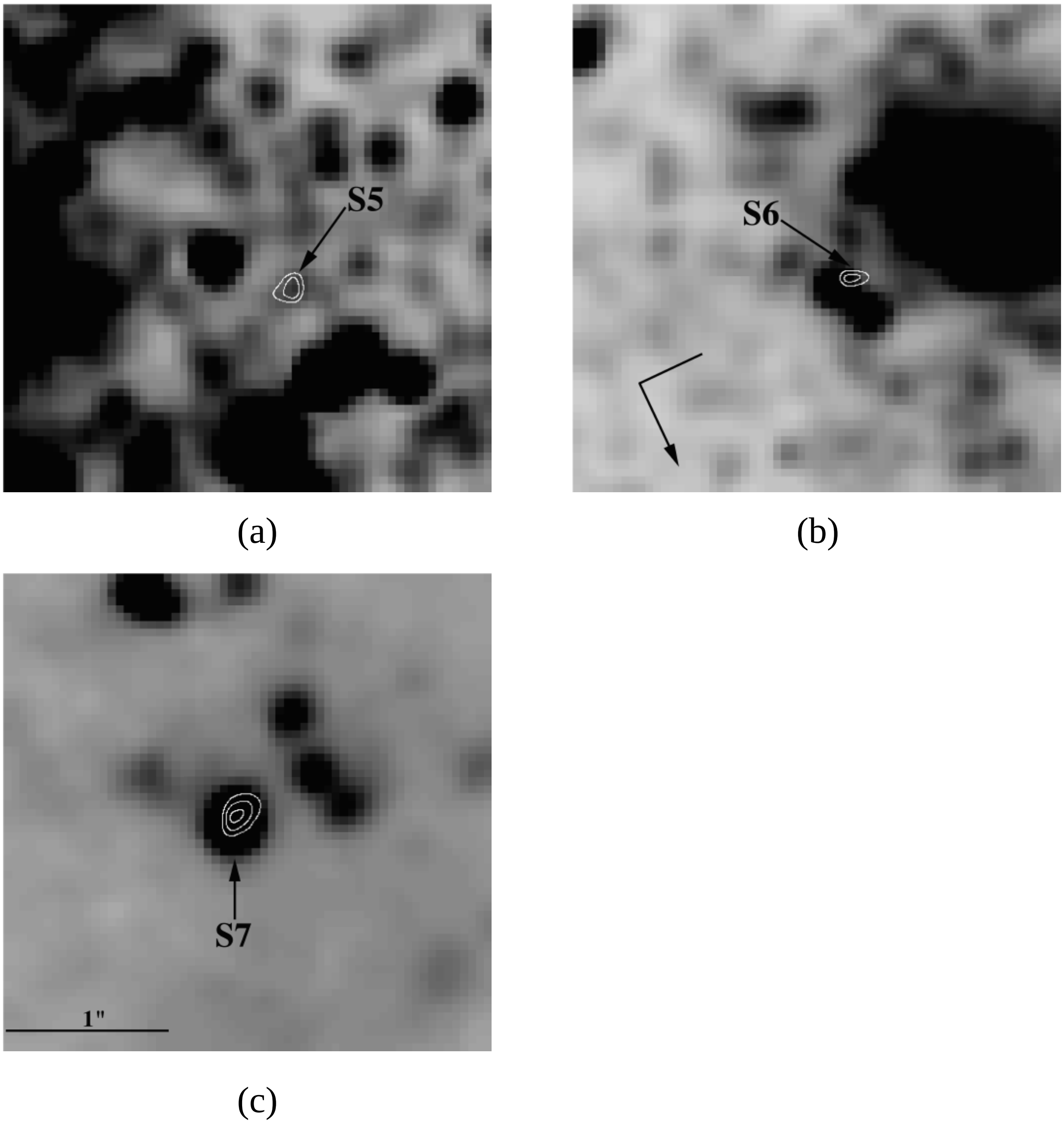

Fig. 4.— “Postage stamp” enlargements of the fields of S objects 5 through 7. The size of each image is $3.''1 \times 3.''1$. The gray-scaled image is F555W and the contours are of the F469N image of the same area. The contours are plotted as the 100%, 80%, 60%, and 40% level of the peak He II emission for that object.

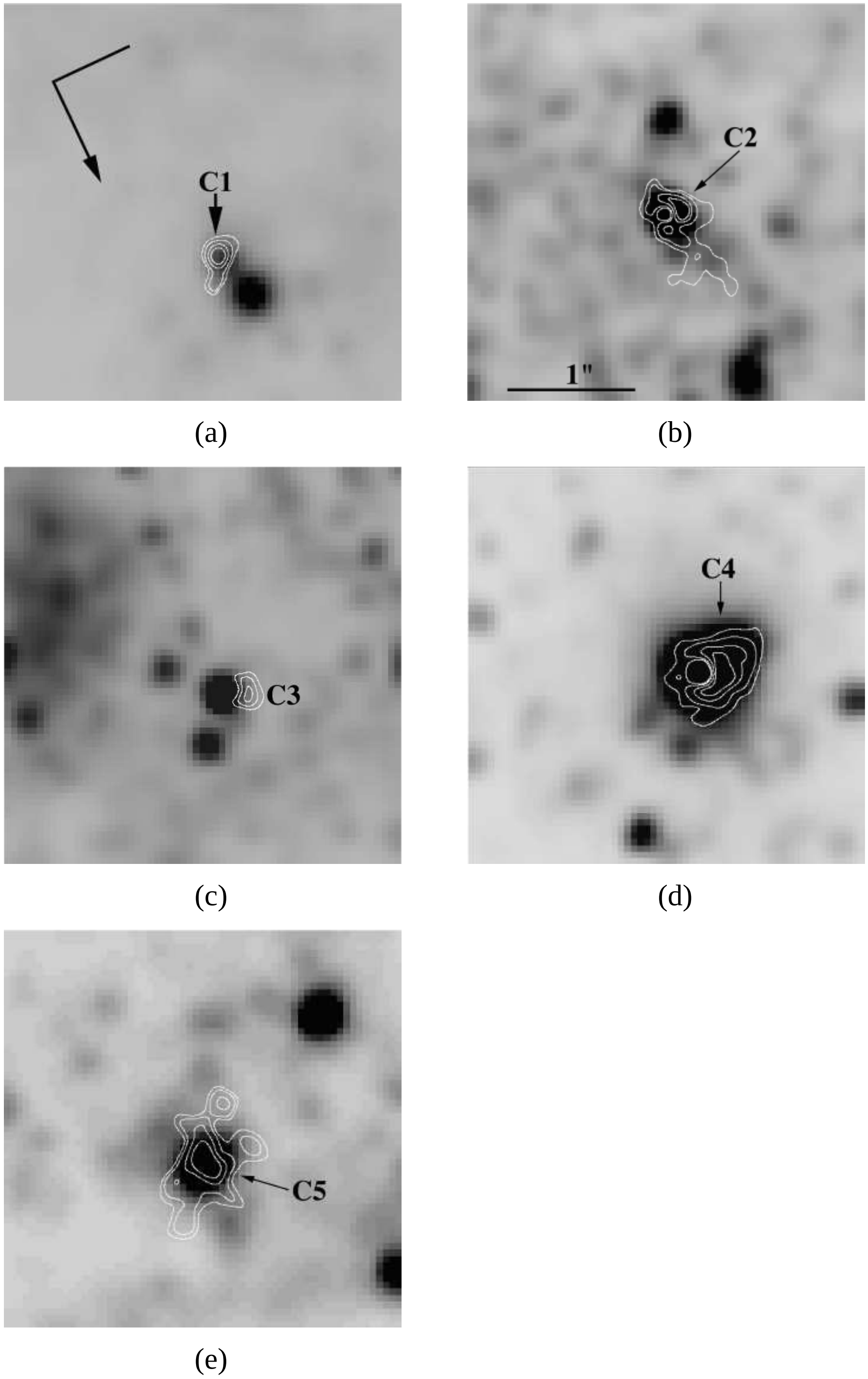

Fig. 5.— "Postage stamp" enlargements of the fields of all C objects. The size of each image is $3''.1 \times 3''.1$. The gray-scaled image is F555W and the contours are of the F469N image of the same area. The contours for all C objects excluding C3 are plotted as the 60%, 40%, 20%, and 10% level of the peak He II emission for that object. C3 has contours at the 100%, 80%, 60%, and 40% level of the peak He II emission.

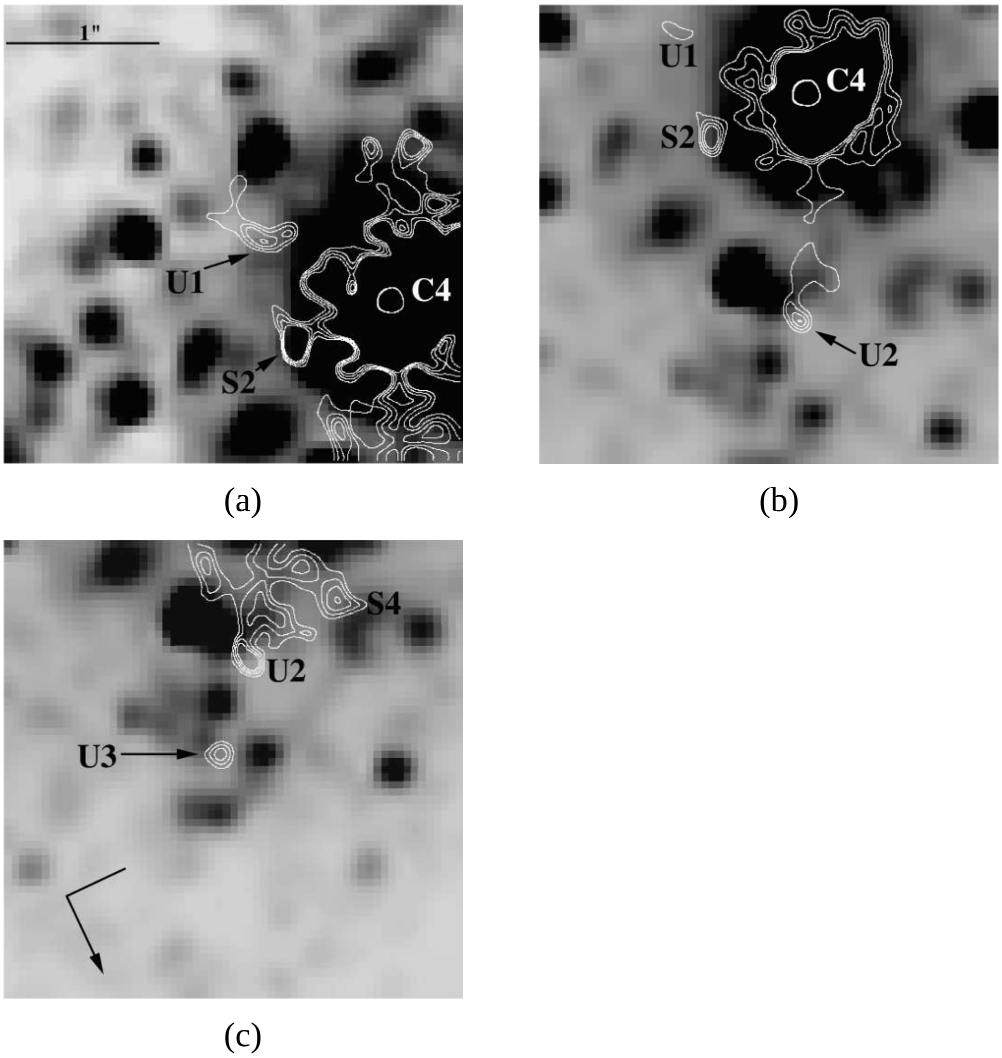

Fig. 6.— “Postage stamp” enlargements of the fields of all U objects. The size of each image is $3''\!.1 \times 3''\!.1$. The gray-scaled image is F555W and the contours are of the F469N image of the same area. The contours are plotted as the 100%, 80%, 60%, and 40% level of the peak He II emission for that object.

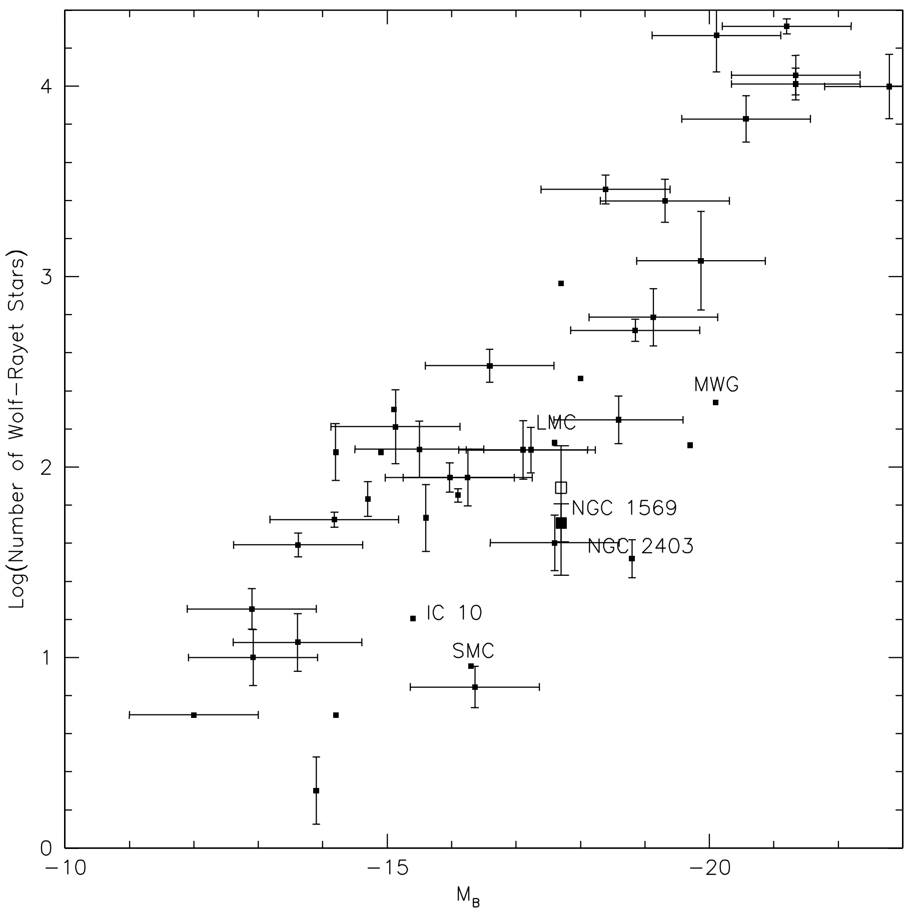

Fig. 7.— Log-Log plot of the number of Wolf-Rayet stars versus the absolute blue magnitude. Wolf-Rayet Numbers for the other galaxies come from the followingreferences: SMC (van der Hucht 1996), LMC (Breysacher, Azzopardi, & Testor 1999), MWG (van der Hucht 1999), IC 10 (Massey et al. 1992), NGC 2403 (Drissen et al. 1999) and others (Vacca & Conti 1992; Guseva et al. 2000). Absolute blue magnitudes were taken from the NASA/IPAC Extragalactic Database (NED), de Vaucouleurs & Pence (1978), Thuan & Martin (1981), Bergvall & Olofsson (1986), Thronson et al. (1990), Kobulnicky et al. (1995), and Guseva et al. (2000). The enlarged, solid NGC 1569 datum point is the detected number of Wolf-Rayet stars. The enlarged, hollow NGC 1569 datum point is the estimated number of Wolf-Rayet stars.

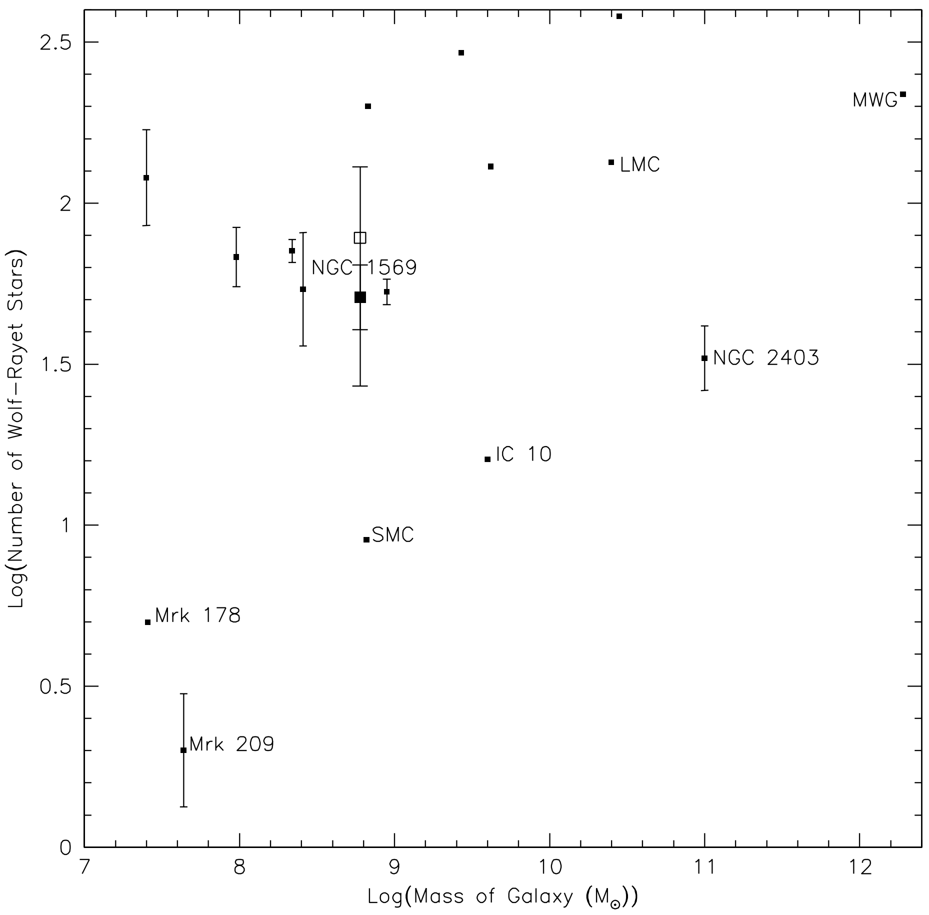

Fig. 8.— Log-Log plot of the number of Wolf-Rayet stars versus the dynamical mass of the galaxy. The number of Wolf-Rayet stars for the other galaxies come from the following references: SMC (van der Hucht 1996), LMC (Breysacher, Azzopardi, & Testor 1999), MWG (van der Hucht 1999), IC 10 (Massey et al. 1992), NGC 2403 (Drissen et al. 1999), Mrk 178 & Mrk 209 (Guseva et al. 2000), and others (Vacca & Conti 1992; Izotov et al. 1997; Guseva et al. 2000). Dynamical masses come from the following sources: SMC (Loiseau & Bajaja 1981), LMC (de Vaucouleurs 1960), NGC 1569 (Stil & Israel 1998), NGC 2403 (Burns & Roberts 1971), MWG (Wilkinson & Evans 1999), IC 10 (Cottrell 1976), Mrk 178 & Mrk 209 (Thuan & Martin 1981), and others (Thuan & Martin 1981; Jackson et al. 1987; Dufour & Hester 1990; Taylor et al. 1993; Kobulnicky et al. 1995).The enlarged, solid NGC 1569 datum point is the detected number of Wolf-Rayet stars. The enlarged, hollow NGC 1569 datum point is the estimated number of Wolf-Rayet stars.

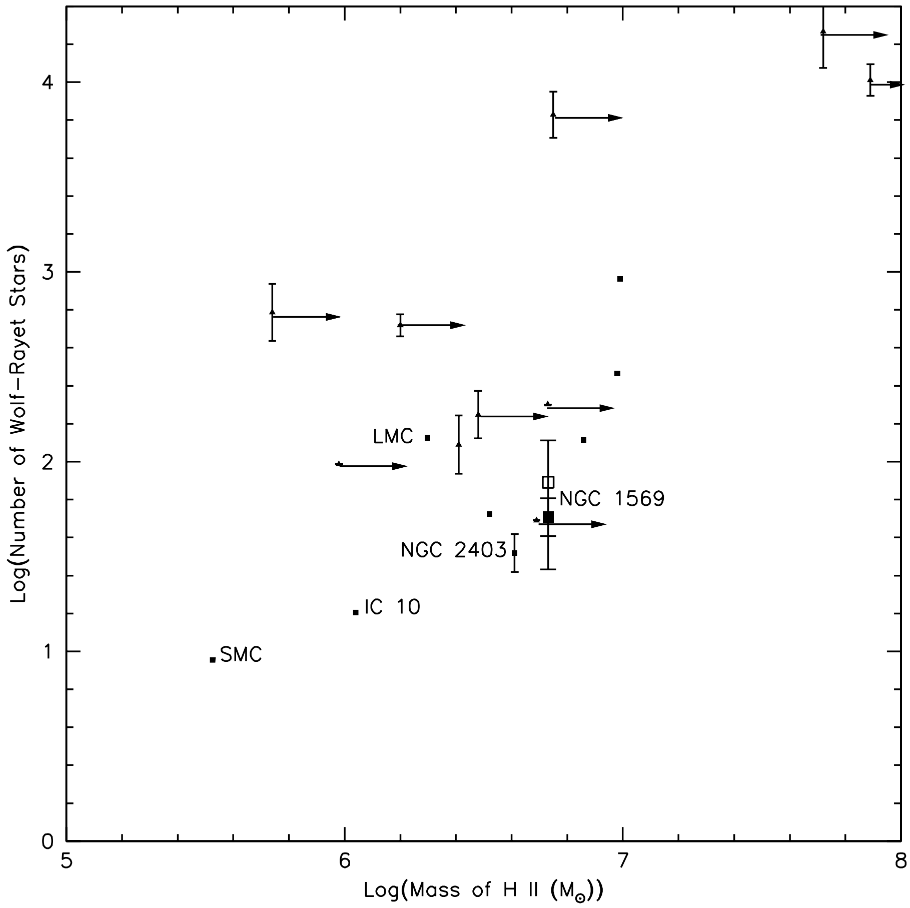

Fig. 9.— Log-Log plot of the number of Wolf-Rayet stars versus the H II mass of the galaxy. Square data points are total measurements of the H II mass. Triangle data points with associated arrows are lower limits of the H II mass computed using data from Guseva et al. (2000) and Viallefond & Goss (1986). Wolf-Rayet Numbers for the other galaxies come from the following references: SMC (van der Hucht 1996), LMC (Breysacher, Azzopardi, & Testor 1999), IC 10 (Massey et al. 1992), NGC 2403 (Drissen et al. 1999) and others (Vacca & Conti 1992; Izotov et al. 1997; Massey & Johnson 1998b; Bransford et al. 1999; Guseva et al. 2000). H II masses were derived using the empirical formula from Kennicutt (1988), which states that the mass of H II equals 1.2×10^5 L(Hα)$\times$ 10^{-39} $M_\odot$. The luminosity of Hα came from the following sources: SMC & LMC (Kennicutt et al. 1995), NGC 1569 (Waller 1991), IC 10 (Thronson et al. 1990), NGC 2403 (Sivan et al. 1990), and others (Viallefond & Goss 1986; Dufour & Hester 1990; van den Broek et al. 1991; Vacca & Conti 1992; Walterbros & Braun 1994; Mendez et al. 1999; Guseva et al. 2000).The enlarged, solid NGC 1569 datum point is the detected number of Wolf-Rayet stars. The enlarged, hollow NGC 1569 datum point is the estimated number of Wolf-Rayet stars.

Table 1. Observational Parameters of HST/WFPC2 New & Archival Data

Filter	Band/ Emission Line	PI	GO-Program Number	Date	Exposure Time (sec)
F469N	He II	Shopbell	8133	23 Sept. 1999	2600
F502N	[O III]	Shopbell	8133	23 Sept. 1999	1500
F547M	Strömgren y	Shopbell	8133	23 Sept. 1999	60
F555W	*WFPC2* V	Hunter	6423	21 Oct. 1998	930
F439W	*WFPC2* B	Leitherer	6111	10 Jan. 1996	11280
F555W	*WFPC2* V	Leitherer	6111	10 Jan. 1996	9720

Table 2. He II Point Sources with an Associated F555W Point Source and No [O III] Point Source

Number Number	R.A. (2000)	Dec (2000)	F_λ (He II)[a]	V[b]	B-V[c]
S1	4 30 48.0	64 51 01.9	2.26 (0.2)[d]	22.0 (0.1)	0.6 (0.1)
S2	4 30 48.2	64 50 59.0	2.98 (0.2)	19.35 (0.04)	–
S3	4 30 48.4	64 50 59.0	0.696 (0.2)	22.8 (0.5)	–
S4	4 30 48.5	64 50 59.2	0.975 (0.1)	21.0 (0.1)	0.5 (0.1)
S5	4 30 48.6	64 50 57.5	1.194 (0.1)	21.3 (0.1)	0.4 (0.1)
S6	4 30 49.0	64 50 53.3	2.20 (0.1)	21.5 (0.2)	0.5 (0.3)
S7	4 30 59.2	64 50 20.6	2.10 (0.1)	22.3 (0.02)	–

[a]F_λ measurements are in the units of 10^{-16} ergs sec^{-1} cm^{-2}

[b]$(V - M_V)_{\rm NGC1569} = 5\log(D) - 5 + A_V = 26.7\pm0.6 + 2.2\pm0.3 = 28.9\pm0.7$; D from Israel (1988) & A_V from Devost, Roy, & Drissen (1997)

[c]$E(B\text{-}V)_{\rm NGC1569} = 0.7 \pm 0.09$ from Devost, Roy, & Drissen (1997)

[d]Numbers in parentheses are 1σ uncertainties.

Table 3. He II Sources with an Associated Star Cluster

Number	R.A. (2000)	Dec (2000)	F_λ (He II)[a]	V[b]	B-V[c]	Area of He II Emission (arcsec^2)
C1	4 30 47.3	64 51 02.1	7.21 (0.1)[d]	17.41 (0.02)	1.44 (0.03)	0.0794
C2	4 30 47.5	64 50 58.3	8.81 (0.1)	18.80 (0.03)	1.08 (0.06)	0.0893
C3	4 30 47.7	64 51 01.4	5.89 (0.1)	19.39 (0.04)	0.37 (0.05)	0.0496
C4	4 30 48.2	64 50 58.5	131.1 (0.2)	15.22 (0.00)	0.23 (0.00)	0.823
C5	4 30 51.5	64 50 48.8	6.95 (0.07)	18.91 (0.02)	–	0.0298

[a]F_λ measurements are in the units of 10^{-16} ergs sec^{-1} cm^{-2}

[b]$(V - M_V)_{\rm NGC1569} = 5\log(D) - 5 + A_V = 26.7 \pm 0.6 + 2.2 \pm 0.3 = 28.9 \pm 0.7$; D from Israel (1988) & A_V from Devost, Roy, & Drissen (1997)

[c]$E(B\text{-}V)_{\rm NGC1569} = 0.7 \pm 0.09$ from Devost, Roy, & Drissen (1997)

[d]Numbers in parentheses are 1σ uncertainties.

Table 4. He II Sources with Neither [O III] Nor F555W Source

Number	R.A. (2000)	Dec (2000)	F_λ (He II)[a]	Area of He II Emission (arcsec^2)
U1	4 30 48.1	64 50 58.5	0.861 (0.2)[b]	0.00992
U2	4 30 48.3	64 50 59.5	1.778 (0.2)	0.0198
U3	4 30 48.4	64 51 00.6	0.767 (0.1)	0.00992

[a]F_λ measurements are in the units of 10^{-16} ergs sec^{-1} cm^{-2}

[b]Numbers in parentheses are 1σ uncertainties.